

Tatajuba: exploring the distribution of homopolymer tracts

Leonardo de Oliveira Martins^{1,*}, Samuel Bloomfield¹, Emily Stoakes², Andrew J. Grant², Andrew J. Page¹ and Alison E. Mather^{1,3}

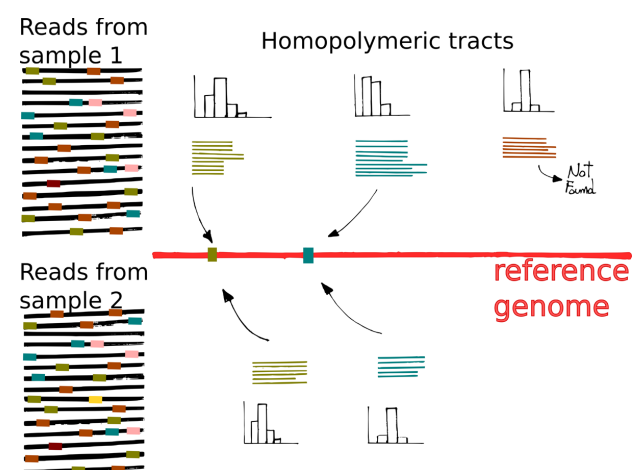
¹Quadram Institute Bioscience, Norwich Research Park, Norwich NR4 7UQ, UK, ²Department of Veterinary Medicine, University of Cambridge, Madingley Road, Cambridge CB3 0ES, UK and ³University of East Anglia, Norwich Research Park, Norwich NR4 7TJ, UK

Received August 02, 2021; Revised November 18, 2021; Editorial Decision December 21, 2021; Accepted January 05, 2022

ABSTRACT

Length variation of homopolymeric tracts, which induces phase variation, is known to regulate gene expression leading to phenotypic variation in a wide range of bacterial species. There is no specialized bioinformatics software which can, at scale, exhaustively explore and describe these features from sequencing data. Identifying these is non-trivial as sequencing and bioinformatics methods are prone to introducing artefacts when presented with homopolymeric tracts due to the decreased base diversity. We present tatajuba, which can automatically identify potential homopolymeric tracts and help predict their putative phenotypic impact, allowing for rapid investigation. We use it to detect all tracts in two separate datasets, one of *Campylobacter jejuni* and one of three *Bordetella* species, and to highlight those tracts that are polymorphic across samples. With this we confirm homopolymer tract variation with phenotypic impact found in previous studies and additionally find many more with potential variability. The software is written in C and is available under the open source licence GNU GPLv3.

GRAPHICAL ABSTRACT



INTRODUCTION

The presence of repetitive DNA bases across bacterial genomes is ubiquitous and is associated with important phenotypic changes, especially in organisms with skewed GC content (1,2). These repetitive regions are known as homopolymeric tracts (HT), they can lead to phase variation; the resultant change can lead to truncation of coding sequences with consequent changes in gene expression and therefore phenotype. Or if the HT occurs in non-coding control regions, it can affect the expression of genes. Identifying and monitoring all HTs in a sample can be challenging due to the large numbers and difficulty in identifying such tracts from sequence data. Since these frameshift events can be common in a population and regulate, or affect, the expression of genes with important phenotypic traits, effort should be directed to identify variation in tract lengths.

To date, evolutionary analyses have focused on single nucleotide polymorphisms (SNPs) and insertions and deletions (indels). In contrast to SNPs, HTs are harder to

*To whom correspondence should be addressed. Tel: +44 1603 255 004; Fax: +44 1603 255 000; Email: Leonardo.de-Oliveira-Martins@quadram.ac.uk

sequence, depend on the GC-content and may lead to biased coverage by current sequencing technologies (3–6). Furthermore, they are problematic to align across samples, since HTs are represented as indels (insertion-deletions) in phylogenetics. With the exception of a few specialist models (7–10), indels are treated as missing data in evolutionary inferences (11–13). They are furthermore challenging to catalogue, unless there is a specific region of interest which can then be curated manually for the presence of HTs. Our proposed algorithm, implemented in the software *tatajuba*, can be applied to any genome with an available annotated reference sequence, and can extract all HTs within the genome while allowing for tract length polymorphism even within a sample. To account for sequencing errors, *tatajuba* conservatively only calls HTs in areas with high read coverage, supported by both strands, and with sufficiently long flanking DNA on each read. The flanking regions must allow for the HT to be uniquely mapped to the reference genome, with length defined by the user, currently limited to less than 32 bp on each side. We consider read coverage in both forward and reverse strands by using a canonical representation of the tracts. The software can optionally be configured at runtime to be less conservative, neglecting the strand bias around HTs, with the risk of an elevated false positive rate of HTs identified or losing the ability to map against the reference in a few cases.

Our objective is to fully describe the distribution of tract lengths for all HTs in a sample, and to compare differences in HT length across a given set of samples. Differences in the variability of HTs across samples can give us information about evolutionary processes (diversity) and phenotype, and can be explicitly modelled. Changes in the tract length can suggest a phenotypic impact, and by providing BED and VCF files specific to the tracts, *tatajuba* facilitates exploring the functional impact of the HT variants. Using the whole distribution across reads, as opposed to assuming a single consensus sequence per sample, allows us to account for minor variants and intra-sample diversity, essential for observing small-scale evolutionary trends and phase variation in clonal populations (14).

We demonstrate the software capabilities on two data sets where the importance of phase variation has been previously described, *Campylobacter* (2) and *Bordetella* (15), but this tool can be applied to any microbial species. The name *tatajuba* (spelled *tatajubá* in Portuguese) comes from the South American hardwood tree *Bagassa guianensis*, meaning ‘yellow fire’ or ‘fire wood’ in Tupi-Guarani.

MATERIALS AND METHODS

The software focuses on describing the tract length distributions across samples, by mapping them to a reference annotated genome and finding those with variability across samples. Given a FASTQ file as input, an HT is found from sequencing reads of nucleotides, and is defined as the same base repeated (e.g. 3 times or more), and flanked by a pair of k-mers, called ‘contexts’. Each context is thus a short DNA segment, between 10 and 32 bp typically, which flanks an HT and contains a rich set of nucleotide sequences. Using these flanking regions to anchor the HT avoids bioinformatic artefacts usually inherent around HTs. We will refer

Table 1. The tract can be variable

DNA segment	Difference from canonical tract
ATTCATCTATCCCCATATCATTGA	Canonical tract
ATTCATCTATCCCATATCATTGA	Tract length polymorphism
ATTCATCTATCCCCATATCGTTGA	Substitution on right context
TTCATCTATGCCCCATATCATTGA	Insertion in left context
TCAATGATATGGGGGATAGATGAAT	DNA segment is reverse complement of canonical

All the following read segments come from the same tract, represented at the top as the ‘canonical’ or exemplary tract (notice that the contexts have fixed size of 10 bases in this example).

to an HT together with its pair of contexts simply as a tract, and we will consider only those tracts that can be mapped to the reference genome – otherwise they are discarded, but can be reported to the user since a large fraction of those can be indicative of an inappropriate choice of reference sequence or sequence contamination.

Furthermore, in the presence of paralogs or, specifically, when the exact same tract is mapped to more than one region in the reference genome, the method chooses the first one in genomic coordinates. To avoid inclusion of sequencing errors, we only consider an exact DNA sequence (i.e. read segment with identical contexts and homopolymer) observed in more than a number of reads fixed by the user (default is 5). Afterwards we can merge these identical DNA segments into a tract if their contexts are similar enough (based on their edit distance) and map to the same location in the reference genome, and their homopolymers are composed of the same base (see Table 1). Specifically, we use the C functions from BWA-aln for single ended reads (16) to map each tract against the reference. Some tracts will not be mapped due to inappropriate reference or contamination, and these are excluded from further analysis. In both cases the tract is not represented in the reference genome of choice (but may map to a different reference). The tracts might also fail to map due to poor aligner performance on low complexity regions, but large flanking regions should minimize this risk.

The tracts are therefore comparable across samples, where we can now create a list of tracts present in at least one sample (with an equivalent region also in the reference). In addition to reporting all identified tracts, we also highlight those that present variability across samples or in relation to the reference genome. This will generate a smaller set of tracts with potentially important biological implications. The measure of dispersion used here to find variable tracts is the absolute range (MAX-MIN). Other measures could be used, for instance the *relative difference of ranges* (similar to the coefficient of range), but it is being used here solely to exclude the tracts that do not change at all between samples. Tracts which are missing from a sample (but found in others) are also considered variable.

Besides the read files for all samples to be analysed, *tatajuba* requires the reference genome both in fasta format and its GFF3 file, such that it can access the annotations harbouring each tract and identify if the tract falls within a coding sequence or not. It works with *prokka*’s GFF3 output (17), which means that the GFF3 file (i) can

contain the fasta sequences, and (ii) can have more than one contig/chromosome/genome. Therefore, a multiple sequence FASTA file can also be provided in addition to the GFF3 file, which renders tatajuba compatible with multiple reference genomes.

For the phylogenetic comparison, we used snippy (<https://github.com/tseemann/snippy>) for generating the core genomes, assuming the same (single) reference genomes as for tatajuba. Using snp-dists (<https://github.com/tseemann/snp-dists>) to generate a distance matrix between the genomes considering only SNPs, we calculated the UPGMA trees with the `hclust()` function for R (18,19). For estimating the variant effects, snpEff was used after normalization and merging with bcftools of the VCF files output by tatajuba (20,21).

Software implementation

The Levenshtein distance is used to decide if contexts from read segments represent the same tract. There are a few cases where the program detects two tracts that map to the exact same location in the reference genome. These cases may reflect a substitution within the homopolymeric region, which renders the flanking regions too dissimilar to be merged by the program. It can also happen when the flanking region includes an HT itself. Two examples are given in Table 2, where the same sample can present both versions of the tract.

The maximum distance allowed can be controlled by the user, with the default being one, but the example above highlights how this information might be useful. By using the distribution of lengths in contrast to their consensus value, we can observe subtle changes in the populations, as for instance a sample where for a particular tract most reads have a length 4 homopolymer, but a few have length 5.

Samples

It has been shown that the HT variation can be used to identify particular phenotypic traits, such as cell shape in *Campylobacter jejuni* (2). We thus analysed 100 *Campylobacter* samples used in (2): 68 of which had a phase variation described in one of the two genes of interest (*pgp1* and *pgp2*), and 32 ‘wild type’ samples, i.e., without a phase variation described in the original paper (list of samples and accession numbers available as Supplementary Tables and at <https://github.com/quadram-institute-bioscience/tatajuba>). We used *C. jejuni* M1 (ASM14870v1) as the reference genome.

Another study described a set of HTs with potential biological relevance and variability across three *Bordetella* species (15). In this study there were no available data to evaluate intra-species variation, but recently many data sets have been deposited in public repositories. We therefore were able to analyse 108 *Bordetella* samples downloaded from ENA (91 *Bordetella pertussis*, 7 *Bordetella parapertussis* and 10 *Bordetella bronchiseptica*), using *B. pertussis* Tohama I (ASM19571v1) as the reference genome. The *B. pertussis* samples come from bioprojects PRJNA348407, PRJNA356412, PRJEB42353 and PRJEB38438 (22–24), while the *B. parapertussis* and *B. bronchiseptica* come from bioproject PRJNA287884 (25). In order to analyse the 108

Bordetella samples, besides the single reference genome we also used a panel of reference genomes composed of a *B. pertussis* Tohama I (ASM19571v1), a *B. parapertussis* 12822 (ASM19569v1) and a *B. bronchiseptica* RB50 (ASM19567v1) for which we have the assembled and annotated genomes.

RESULTS

From each sample, we selected all tracts with homopolymeric lengths of 3 bp or more, which were present in at least 8 reads. We assumed a context of 28 bp on each side, and merged those with a Levenshtein distance smaller than 2, correcting for strand bias by removing HTs not observed in both directions. For these parameters, we found a total of 179 691 tracts for *Bordetella* and 144 119 tracts for the *Campylobacter* data set, which could be mapped to their single reference genomes. If we use a panel of reference genomes, then the number of tracts found for the *Bordetella* data set jumps to 496 293. The numbers for each individual sample are shown in Figure 1, where we can see that (i) both single reference data sets have comparable numbers of mapped HTs: around 140k tracts for most samples for both data sets, although the variation is higher for *Bordetella*; (ii) when a panel of references is used, several samples increase their number of mapped tracts, showing the benefit of adding references similar to the samples; (iii) however, even when using the wrong species (Figure 1, middle panel) the *B. parapertussis* and *B. bronchiseptica* did have more than half their HTs mapped to the *B. pertussis* reference, indicating some robustness to the reference choice; (iv) the unmapped tracts are a combination of the underlying evolutionary processes (e.g. novel mutations) and artefacts like technical contamination or poor choice of the reference genome, as we saw above from the inclusion of more references. Another artefact is confirmed by running the software without strand bias correction, where the number of unmapped tracts increases without an improvement on the number of mapped reads (result not shown). The exception is sample ERR4176311, a *B. pertussis* Tohama I delta-BP3063 mutant from (24), where almost all tracts are seen in only one strand: the 139 348 tracts mapped to the reference decrease to only 875 once we remove tracts not seen on both strand directions. This sample was removed from subsequent analyses. When the genome sizes are taken into account (1.6Mb for *Campylobacter* against 4Mb of *Bordetella*) then the frequency of HTs in *Campylobacter* is almost twice as high as in *Bordetella*.

Tatajuba analysed the 100 *Campylobacter* samples in 12 min and the 108 *Bordetella* in 15 min (single or multi-reference), using a computer with 48 cores and using less than 30GB. Currently we exclude tracts that cannot be mapped to the reference. In the *Campylobacter* dataset, we found 41 108 variable tracts (with variable length distributions or missing from one of the samples), of which 36 605 were annotated, that is, belonged to a gene or RNA. From the *Bordetella* data set, after removing sample ERR4176311 and using a single reference genome, we found 123 686 variable tracts, 106 206 of which were in annotated regions. By using the average length of an HT as a feature, we can cluster all samples based on how similar their sets of tracts are (in

Table 2. Examples where tatajuba finds more than one tract mapping to the same location in the reference genome

Tracts mapping to position 1269169 (cds-WP.002877328.1)
 GGTGTTTTTAAGATGATAAGCATGCTTTGGGTCAGCAAGTGAAGAATTGACAC ← reference
 GGTGTTTTTAAGATGATAAGCATGCTTTGGGTCAGCAAGTGAAGAATTGACAC ← tract tid.112808
 TGGTGTTTTAAGATGATAAGCATGCTTTGGATCAGCAAGCGAAGAATTGACAC ← tract tid.112807
 Tracts mapping to position 127480 (unannotated)
 TTTCTACTAAAATATCCTTTGTAGTTTTATCATTCTTAAAACAAATTCATT ← reference
 TTTCTACTAAAATATCCTTTGTAGTTTTATCATTCTTAAAACAAATTCATT ← tract tid.113353
 CTTACTAAAATATCCTTTGTAGTTGTTTTATCATTCTTAAAACAAATTCATT ← tract tid.113354

The polymeric tract is represented in bold, and differences in context (flanking regions) are highlighted in italics. The top panel shows an example where substitutions on the flanking regions and a (HT-related) deletion are responsible for the classification, while the bottom panel shows potentially successive insertions, with the 'G' disrupting the otherwise increased poly-T.

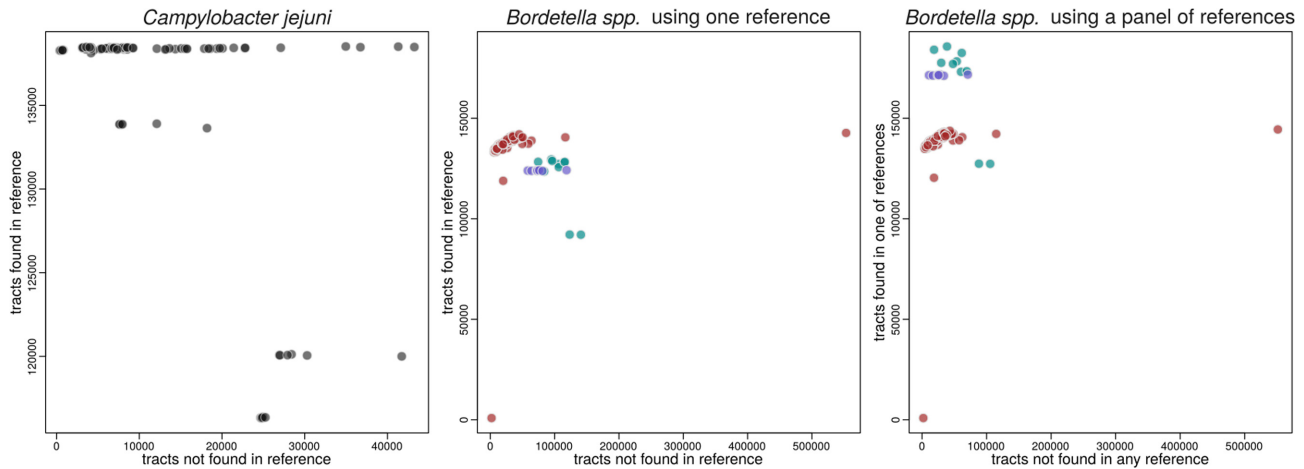


Figure 1. Number of tracts that could be mapped or not to the reference genomes per sample, for the *Campylobacter* (left) and *Bordetella* (middle) datasets using one reference genome, as well as for the same *Bordetella* dataset but using a panel of three reference genomes (right). Each point represents a sample, where some HTs can be mapped back to the reference genome (y axis) and some HTs cannot be mapped (x axis). The total number of HTs found by tatajuba are the sum of the x and y axes for each sample. For the *Bordetella* datasets (middle and right panels), the colours represent samples from different species (red for *B. pertussis*, green for *B. bronchiseptica*, and purple for *B. parapertussis*).

terms of their average length profile). The results are shown in Figure 2, where we see that such clustering is in agreement with the isolate names for *Campylobacter*, which indicate their strains M1, NCTC11168, 81116 or 81-176 (2). And in particular when using a panel of references, the *Bordetella* samples are monophyletic. We will discuss more about the phylogenetic agreement in the next section.

We furthermore measured the variability of each tract across samples, and visualized them along the genome (Figure 3). In this figure, the variability is represented as the maximum difference between tract lengths across samples, where we can see it is not unusual to observe tracts where samples have a length difference higher than 4, for instance. This dispersion measure is currently used only to exclude HTs with no variation at all across samples, but as we see it gives an overview of highly variable tracts. Other measures can be implemented, which are more robust to outliers as for instance the interquartile range, or are based on the length distribution within a sample instead of a point estimate as cross-bin distances (26). Furthermore, length changes in multiples of three (a codon) might have a lower impact than those potentially changing the reading frame.

In (2), 18 modifications in genes *pgp1* and *pgp2* were described which were associated with rod-shaped *C. jejuni* (Table 1 of that paper). Of these, 12 involve a change in the length of the homopolymer tract. In Figure 4 we observe

that most mutations (10 out of 12) previously described leading to tract length modifications (2) are also found by tatajuba. The correspondence between the changes found in (2) and in tatajuba are shown in Table 3. Some (2 out of 12) are missing since we limited the search to homopolymers of length 3 or higher. Interestingly, tatajuba misses the changes originally reported in locations 1268739 and 1268827 from 3A to 2A. Instead, it reports 3A for all samples, since it stores the distribution of homopolymers truncated at 3: even if the 2A (dimer) form is more frequent than the trimer 3A (and would therefore be the consensus), tatajuba does not keep track of dimers. Upon further inspection (by allowing dimers, results not shown) we confirmed this is the case for 1268739. For 1268827 and other cases where tatajuba does not detect the HT change for some samples, like locations 1268899 and 1268944, may be due to low tract coverage or missing context from raw reads (see also Figure 7 below for an example where there is insufficient context around a given HT).

For the *C. jejuni* data set, we found 5445 variants involving the HT sites from the VCF files generated by tatajuba. This number is well below the 41k variable tracts, since it does not account for missing tracts: HTs identical between the reference and the sample are not reported in the VCF file, as well as HTs which were not found in the sample. These variants generated a total of 10 115 functional an-

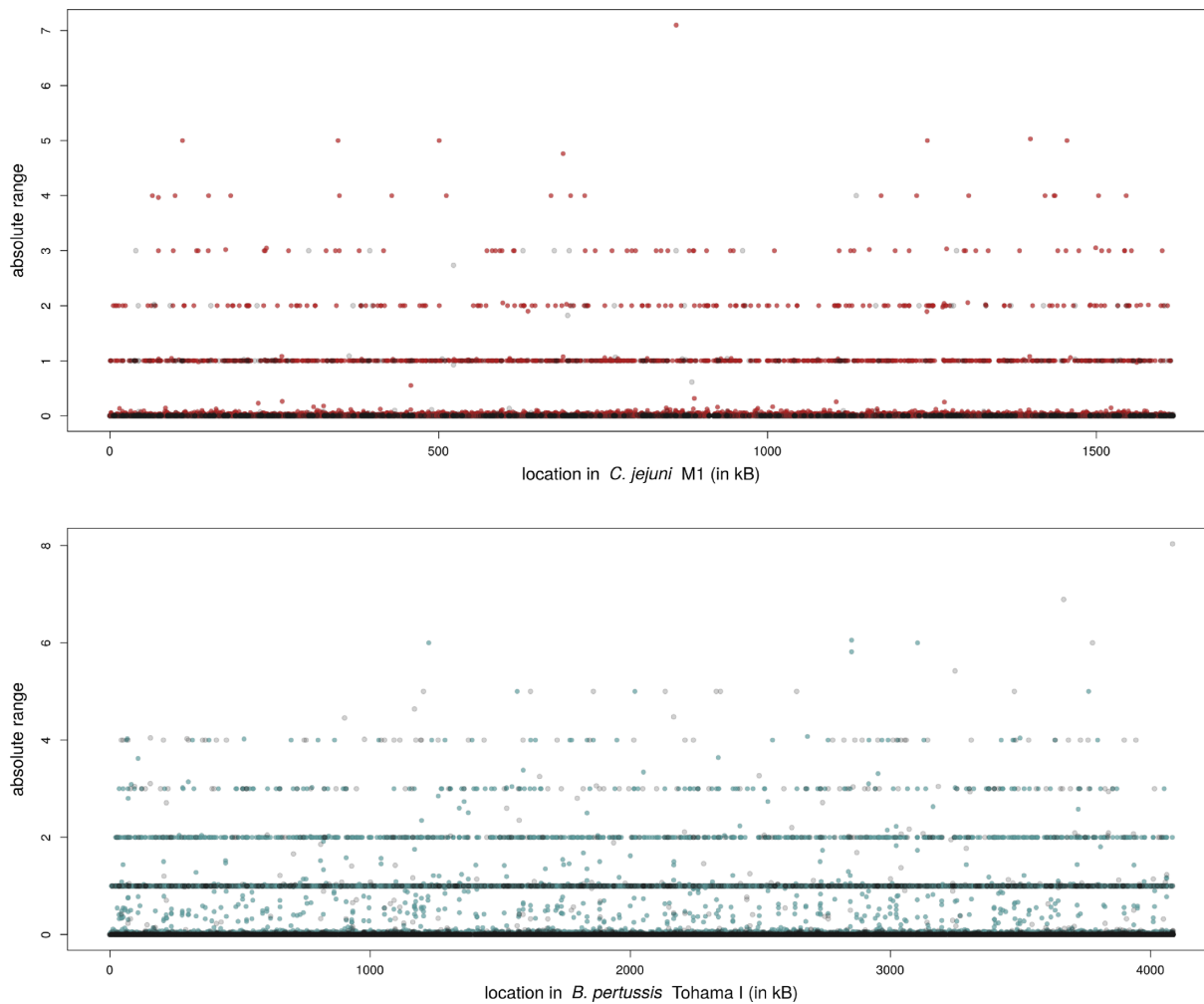


Figure 3. Tract length ranges (maximum minus minimum values across samples) across the reference genome of the two example data sets. Blue or red dots represent tracts in an annotated region while grey dots are not annotated. The tract length is estimated through the average length over reads, and only variable tracts are shown (i.e. those with range higher than zero).

tinguish between distinct topologies (11–13). However, if we account for the indel patterns within each HT (the coloured segments), then we can infer which genomes are more similar, assuming that HT-related indels are reliable, i.e. less likely to be alignment artefacts (10,30,31).

To show the effect of incorporating the HT signal on our data sets, we compared tatajuba with a traditional phylogenomic inference, using snippy to create the core genomes from both data sets. Snippy tracks all nucleotide variants with respect to a reference genome (same ones as used for tatajuba, in our case) while discarding insertions. While tatajuba identified 38 937 distinct HT start locations, snippy found 34 644 SNP locations, since it excludes insertions with respect to the reference. In Figure 6B, we see how tatajuba recovers the same clusters as snippy, but with higher resolution as represented by the longer branch lengths and fewer polytomies. This becomes evident when we compare directly the pairwise distances between samples using HTs and SNPs (Figure 6C): there is overall good correspondence, as expected, but especially for the most similar sample pairs, there is no observable SNP differences despite subtle differences in their HT lengths.

The same result was observed for the *Bordetella* sequences when we use one reference genome, including the paraphyly of *B. bronchiseptica* (results not shown). For this comparison there were 120 201 SNPs and 115 528 distinct variable HT locations. Notice that the number of distinct HT locations is smaller than the total number of variable HTs since some map to the same location (Table 2). The multi-genomic panel of references cannot be compared with snippy, however Figure 2 alone shows the phylogenetic improvement of using a panel instead of a single reference: the monophyly is recovered, and the longer branches further indicate a higher phylogenetic resolution (32).

DISCUSSION

One future direction is to explore the HTs explicitly as phylogenetic markers (30), for instance by extending an alignment from their flanking regions, and combining it with a continuous trait model for the HT lengths (33). The HTs can be rapidly identified across samples, and as we observed carry evolutionary information, although we are only scratching the surface of its potential in

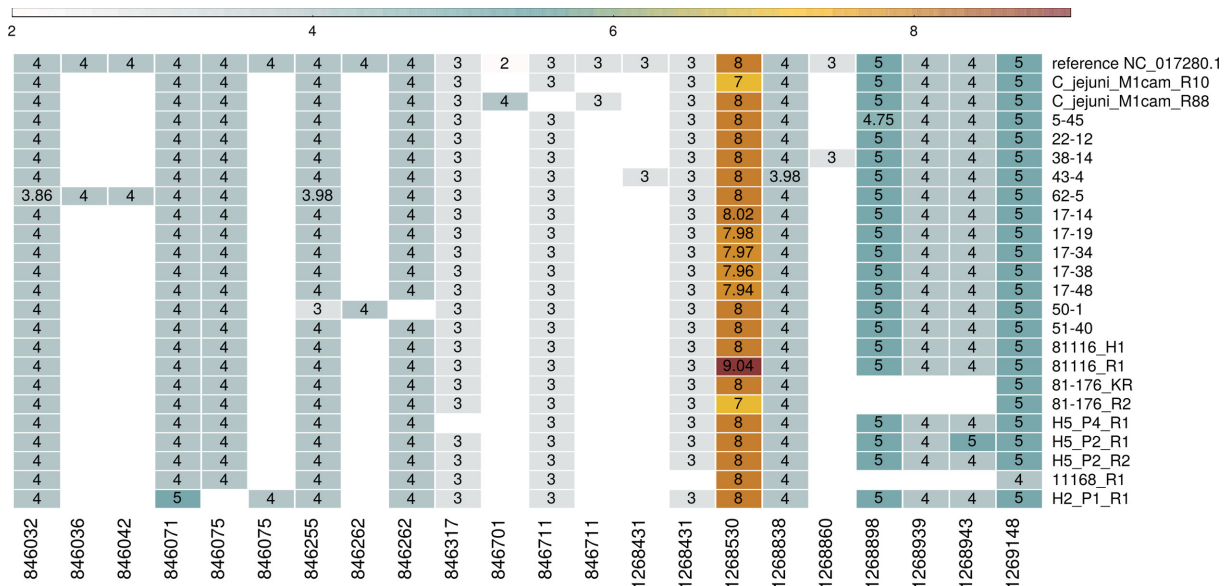


Figure 4. Average tract length for selected *Campylobacter* samples, over genes *pgp1* (from 1268323 to 1269717) and *pgp2* (846020 to 846997) for tracts described in (2). Rows correspond to samples, and columns are the genomic location of the HTs—only variable tracts are shown, i.e. if a tract has same length over all samples, then its column is excluded. The same location appears more than once for cases where tatajuba decides that the contexts are too distinct even if mapping to the same location in the reference genome. Tract lengths smaller than three were not considered by tatajuba and therefore are absent (empty cells).

Table 3. Correspondence between HT length modification found here and in (2)

Location in (2)	Location in tatajuba	change	Samples in Figure 4 where change is observed	Confirmed by tatajuba	Observations
846037 (pgp2)	846032	4 T > 3 T	62–5	Y	
846075 (pgp2)	846075	4 A > 3 A	H2_P1_R1	Y	
846256 (pgp2)	846255	4 A > 3 A	50–1	Y	62–5 and 17–19 show variability
846319 (pgp2)	846317	3 A > 2 A	H5_P4_R1	Y	
846702 (pgp2)	846701	2 G > 4 G	C_jejuni_M1cam_R88	Y	
1268531 (pgp1)	1268530	8 A > 7 A	C_jejuni_M1cam_R10, 81–176_R2	Y	
1268531 (pgp1)	1268530	8 A > 9 A	81116_R1	Y	
1268739 (pgp1)	1268738	3 A > 2 A		N	All samples have length of 3 in tatajuba
1268827 (pgp1)	1268826	3 A > 2 A		N	All samples have length of 3 in tatajuba
1268899 (pgp1)	1268898	5 T > 4 T	5–45	Y/N	Not found in previously reported 17–48; 5–45 is only partial
1268944 (pgp1)	1268943	4 A > 5 A	H5_P2_R1	Y/N	Tract is absent in some samples
1269149 (pgp1)	1269148	5 A > 4 A	11168_R1	Y	

The location shown corresponds to the beginning of the homopolymer, with tatajuba starting at zero (instead of one). Tract lengths smaller than 3 were not recorded and thus appear as ‘absent’.

this manuscript. By exhaustively exploring populations of genomes for their presence, we may find regions of phylogenetic importance. The software allows for multiple genome annotation and therefore can work with several reference genomes.

Tatajuba can be used to help infer the phenotypic effect of tract length variations, by finding those in coding regions and by describing the change in tract length — in coding regions, we expect frameshift mutations to have a higher impact than a tract length difference of multiples of three. Tatajuba outputs a BED file describing the location in the chromosomes involved in a homopolymeric tract, which can be used in standard workflows, with established variant callers. It also generates a VCF file for each sample, re-

stricted to the HT regions and compatible with variant effect prediction tools.

Strand bias, where reads from the forward strand disagree with reads from the reverse strand, are more common around homopolymeric regions (34–36). Although less affected than other technologies, Illumina sequencing can generate spurious indels within HTs (37–39), especially for HT lengths longer than 14 bp (40,41), and it was estimated to affect up to 1% of the genes in a metagenomic data set (42). A recent survey showed that up to 5.3% of all Illumina errors are related to homopolymers of length 3 or more (43). To correct for the length errors induced by strand bias, tracts present in only one strand can be flagged (44), or a filter can be added to exclude length disparities associated

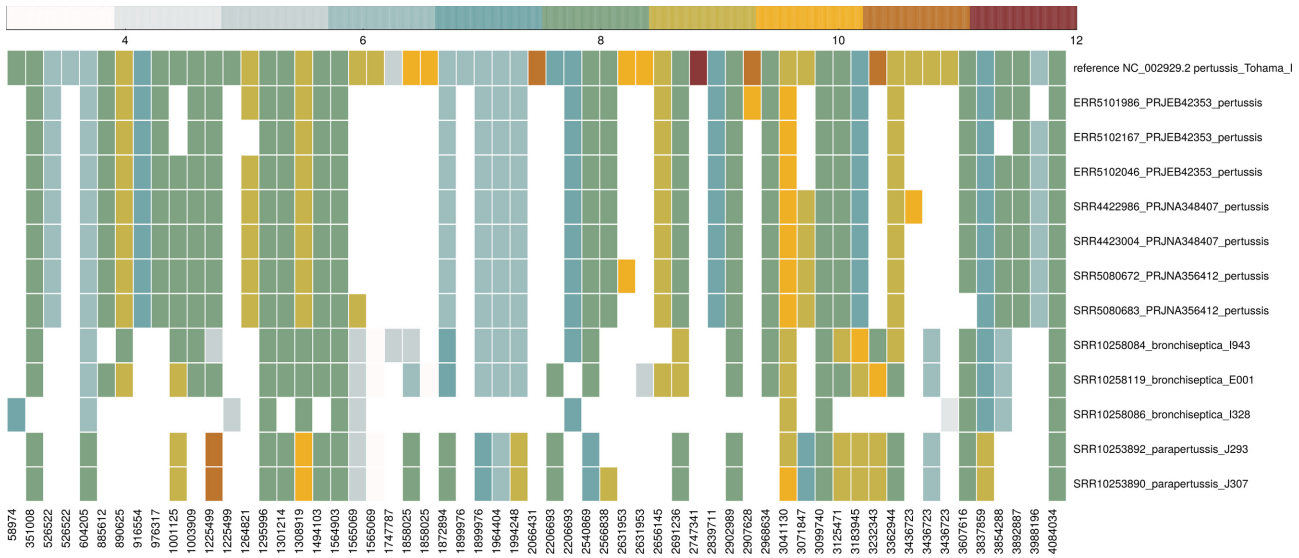


Figure 5. Average tract length for selected *Bordetella* samples, over regions reported in (15). The samples were arbitrarily selected for display purposes, to show the variety of tract lengths.

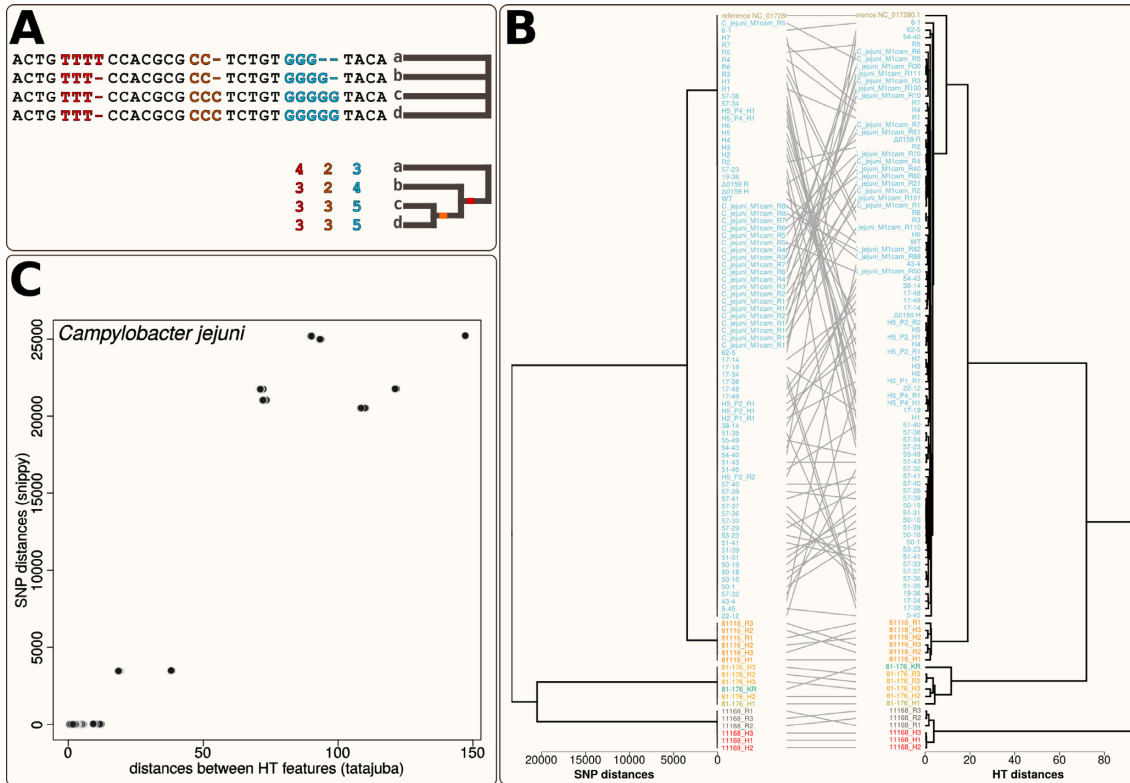


Figure 6. Comparison between sample distances using SNP differences or average HT length profiles for the *Campylobacter* data set. (A) Schematic example of four sequences a, b, c, d having zero SNPs (top) which nonetheless are different, once their homopolymeric tract lengths (coloured numbers) are taken into account. The coloured branches represent putative HT length changes. (B) Tanglegram comparing the UPGMA dendrograms from the distance matrices if we use the number of SNP differences (left) or the Euclidean distance between their average tract length profiles (right). The samples are coloured according to their HT-based clustering. (C) Direct comparison between the pairwise distance matrices, where each point represents an element of the matrix, i.e. a sample pair, using SNPs (y axis) or HTs (x axis).



Figure 7. Search for a specific homopolymer tract using raw reads. The HT reported in (15) has 15 Gs in location 147886 of the *B. pertussis* Tohama I genome. A loose text search for sequence GGGGGGGGGGACGGCC (and its reverse complement GGCCGTCCCCCCCC) returns the reads above for five samples (ten paired end files), with the search text in red. Each sample read has fewer than five valid tracts.

with the strand (34). Tatajuba only considers tract lengths observed on both strands. It has been observed that error correction algorithms might introduce errors around HTs (5), although alternatives exist, in particular quality-score-based error removal (5,45).

BWA-aln is optimized for short reads and has very good performance when the read is similar to the reference genome except for HTs at the end of the alignment (46). However, it fails to map reads with lower matches, unlike mappers which can spuriously return random mappings (46). BWA-aln is thus well suited for tatajuba: in our case the HT is never at the end of the alignment, since it is flanked by conserved sequences, and we assume the presence of a close reference genome.

It is important to keep in mind that our procedure is based on raw reads (samples), and reports HTs which were observed in these samples. This explains why tatajuba could not find the HT reported at BP0146 (genome location 174886) even without accounting for strand bias. In Figure 7, we show a list of all reads from five samples potentially containing the HT, as defined by a small stretch of the poly-G followed by a short flanking region of 6 bases. There we see that this HT is likely to be rejected by tatajuba since it does not have sufficient context (i.e. flanking regions) or its coverage depth is too low.

It is also important to note that tatajuba compares the HTs from each sample to a set of common reference genomes and thus the comparison between samples from different species is automatic, that is, we don't need to map between reference genomes as in (15).

CONCLUSION

HTs are widespread in many bacterial species, and variation in HT length can regulate gene expression. In both bacterial species examined here, HTs were found in large numbers, rendering the task of merely identifying such tracts unmanageable without automation. Clearly, with this number of HTs, an automatic/systematic way of investigating variation is required, which currently does not exist even for assembled genomes. Even when our analyses relied on a single reference genome, we show how we can have meaningful results when several species are analysed together. Tatajuba provides a huge scope for identifying potential genetic and therefore phenotypic variation which has thus far not yet been explored systematically. It therefore facilitates the discovery of important biological insights. Tatajuba cannot solve the coverage bias induced by some sequencing tech-

nologies towards HTs, but it excludes tracts with low depth and within reads without enough context, for instance those at the end of the read, without a flanking region.

Some sequencing platforms are sensitive to homopolymers, which can induce indel errors. For instance, MiSeq can find the correct HT length more often than the Ion Torrent PGM or the 454 GS Junior (37). When the HT leads to sequencing mistakes, reads from the forward strand may produce a HT length distinct from reads from the reverse strand – which would be summarized by tatajuba through the length distribution. We cannot fully eliminate systematic bias from sequencing and bioinformatics, but we can limit it. Additionally, tatajuba can be used as a quality control tool to identify these systematic bias issues. It should be used whenever any sequencing method, technology, or library preparation is being updated on a standard set of bacteria.

DATA AVAILABILITY

Tatajuba is available under the open source GNU GPL 3 licence from <https://github.com/quadram-institute-bioscience/tatajuba>. The software is written in ANSI C (C11 standard with GNU extensions), validated using unit tests and packaged for autotools. The software is also available on bioconda, with Docker and singularity images. The samples used in this study are from public databases (e.g. <https://www.ebi.ac.uk/ena>), and are listed in the Supplementary Tables and in <https://github.com/quadram-institute-bioscience/tatajuba/tree/master/docs>.

SUPPLEMENTARY DATA

Supplementary Data are available at NARGAB Online.

ACKNOWLEDGEMENTS

The authors gratefully acknowledge the support of the Biotechnology and Biological Sciences Research Council (BBSRC), and the two anonymous reviewers, who greatly improved the manuscript.

FUNDING

BBSRC Institute Strategic Programme Microbes in the Food Chain [BB/R012504/1 and its constituent projects BBS/E/F/000PR10348 (Theme 1, Epidemiology and Evolution of Pathogens in the Food Chain),

BBS/E/F/000PR10349 (Theme 2, Microbial Survival in the Food Chain) and BBS/E/F/000PR10352 (Theme 4, Research Infrastructure)]; Quadram Institute Bioscience BBSRC funded Core Capability Grant [BB/CCG1860/1].
Conflict of interest statement. None declared.

REFERENCES

- Orsi, R.H., Bowen, B.M. and Wiedmann, M. (2010) Homopolymeric tracts represent a general regulatory mechanism in prokaryotes. *BMC Genomics*, **11**, 102.
- Esson, D., Mather, A.E., Scanlan, E., Gupta, S., de Vries, S.P.W., Bailey, D., Harris, S.R., McKinley, T.J., Méric, G., Berry, S.K. *et al.* (2016) Genomic variations leading to alterations in cell morphology of *Campylobacter* spp. *Sci. Rep.*, **6**, 38303.
- Modlin, S.J., Robinhold, C., Morrissey, C., Mitchell, S.N., Ramirez-Busby, S.M., Shmaya, T. and Valafar, F. (2021) Exact mapping of illumina blind spots in the mycobacterium tuberculosis genome reveals platform-wide and workflow-specific biases. *Microb. Genom.*, **7**, mgen000465.
- Feng, W., Zhao, S., Xue, D., Song, F., Li, Z., Chen, D., He, B., Hao, Y., Wang, Y. and Liu, Y. (2016) Improving alignment accuracy on homopolymer regions for semiconductor-based sequencing technologies. *BMC Genomics*, **17**, 521.
- Heydari, M., Miclotte, G., Van de Peer, Y. and Fostier, J. (2019) Illumina error correction near highly repetitive DNA regions improves de novo genome assembly. *BMC Bioinformatics*, **20**, 298.
- Iványi, G., Madar, L., Dzsudzsák, E., Koczok, K., Kappelmayer, J., Krulisova, V., Macek, M., Horváth, A. and Balogh, I. (2018) Analytical parameters and validation of homopolymer detection in a pyrosequencing-based next generation sequencing system. *BMC Genomics*, **19**, 158.
- Bouchard-Côté, A. and Jordan, M.I. (2013) Evolutionary inference via the poisson indel process. *Proc. Natl. Acad. Sci. U.S.A.*, **110**, 1160–1166.
- Thorne, J.L., Kishino, H. and Felsenstein, J. (1992) Inching toward reality: an improved likelihood model of sequence evolution. *J. Mol. Evol.*, **34**, 3–16.
- Baptiste, E. and Philippe, H. (2002) The potential value of indels as phylogenetic markers: position of trichomonads as a case study. *Mol. Biol. Evol.*, **19**, 972–977.
- Ashkenazy, H., Cohen, O. and Pupko, T. Huchon, D. (2014) Indel reliability in indel-based phylogenetic inference. *Genome Biol. Evol.*, **6**, 3199–3209.
- Donath, A. and Stadler, P.F. (2018) Split-inducing indels in phylogenomic analysis. *Algorithms Mol. Biol.*, **13**, 12.
- Denton, J.S.S. and Wheeler, W.C. (2012) Indel information eliminates trivial sequence alignment in maximum likelihood phylogenetic analysis. *Cladistics*, **28**, 514–528.
- Dwivedi, B. and Gadagkar, S.R. (2009) Phylogenetic inference under varying proportions of indel-induced alignment gaps. *BMC Evol. Biol.*, **9**, 211.
- van der Woude, M.W. and Bäuml, A.J. (2004) Phase and antigenic variation in bacteria. *Clin. Microbiol. Rev.*, **17**, 581–611.
- Gogol, E.B., Cummings, C.A., Burns, R.C. and Relman, D.A. (2007) Phase variation and microevolution at homopolymeric tracts in *Bordetella pertussis*. *BMC Genomics*, **8**, 122.
- Li, H. and Durbin, R. (2009) Fast and accurate short read alignment with burrows-wheeler transform. *Bioinformatics*, **25**, 1754–1760.
- Seemann, T. (2014) Prokka: rapid prokaryotic genome annotation. *Bioinformatics*, **30**, 2068–2069.
- Everitt, B.S., Landau, S., Leese, M. and Stahl, D. (2011) In: *Cluster Analysis*. 5th edn. Wiley.
- R Core Team (2021) R: a language and environment for statistical computing. *r foundation for statistical computing*.
- Cingolani, P., Platts, A., Wang, L.L., Coon, M., Nguyen, T., Wang, L., Land, S.J., Lu, X. and Ruden, D.M. (2012) A program for annotating and predicting the effects of single nucleotide polymorphisms, snpeff: SNPs in the genome of *Drosophila melanogaster* strain w1118; iso-2; iso-3. *Fly*, **6**, 80–92.
- Danecek, P., Bonfield, J.K., Liddle, J., Marshall, J., Ohan, V., Pollard, M.O., Whitwham, A., Keane, T., McCarthy, S.A., Davies, R.M. *et al.* (2021) Twelve years of SAMtools and BCFtools. *Gigascience*, **10**, giab008.
- Octavia, S., Wu, S.Z., Kaur, S., Valinsky, L., Marva, E., Moran-Gilad, J. and Lan, R. (2017) Whole-genome sequencing and comparative genomic analysis of *Bordetella pertussis* isolates from the 2007–2008 epidemic in Israel. *J. Infect.*, **74**, 204–207.
- Marchand-Austin, A., Tsang, R.S.W., Guthrie, J.L., Ma, J.H., Lim, G.H., Crowcroft, N.S., Deeks, S.L., Farrell, D.J. and Jamieson, F.B. (2017) Short-Read whole-genome sequencing for laboratory-based surveillance of *Bordetella pertussis*. *J. Clin. Microbiol.*, **55**, 1446–1453.
- Novák, J., Jurnečka, D., Linhartová, I., Holubová, J., Staněk, O., Štípl, D., Dienstbier, A., Večerek, B., Azevedo, N., Provazník, J. *et al.* (2020) A mutation upstream of the *rplN-rpsD* ribosomal operon downregulates *Bordetella pertussis* virulence factor production without compromising bacterial survival within human macrophages. *mSystems*, **5**, e00612-20.
- Weigand, M.R., Peng, Y., Batra, D., Burroughs, M., Davis, J.K., Knipe, K., Loparev, V.N., Johnson, T., Juieng, P., Rowe, L.A. *et al.* (2019) Conserved patterns of symmetric inversion in the genome evolution of *Bordetella* respiratory pathogens. *mSystems*, **4**, e00702-19.
- Pele, O. and Werman, M. (2010) In: *The Quadratic-Chi Histogram Distance Family*. Computer Vision – ECCV 2010, https://link.springer.com/chapter/10.1007/978-3-642-15552-9_54.
- Miklós, I., Lunter, G.A. and Holmes, I. (2004) A ‘Long indel’ model for evolutionary sequence alignment. *Mol. Biol. Evol.*, **21**, 529–540.
- De Maio, N. (2021) The cumulative indel model: fast and accurate statistical evolutionary alignment. *Syst. Biol.*, **70**, 236–257.
- Waddell, P.J. (2005) Measuring the fit of sequence data to phylogenetic model: allowing for missing data. *Mol. Biol. Evol.*, **22**, 395–401.
- Gupta, R.S. (2001) The branching order and phylogenetic placement of species from completed bacterial genomes, based on conserved indels found in various proteins. *Int. Microbiol.*, **4**, 187–202.
- Nagy, L.G., Kocsubé, S., Csanádi, Z., Kovács, G.M., Petkovits, T., Vágvolgyi, C. and Papp, T. (2012) Re-mind the gap! Insertion-deletion data reveal neglected phylogenetic potential of the nuclear ribosomal internal transcribed spacer (ITS) of fungi. *PLoS One*, **7**, e49794.
- de Oliveira Martins, L., Page, A.J., Mather, A.E. and Charles, I.G. (2020) Taxonomic resolution of the ribosomal RNA operon in bacteria: implications for its use with long-read sequencing. *NAR Genom. Bioinform.*, **2**, lqz016.
- Levy Karin, E., Wicke, S., Pupko, T. and Mayrose, I. (2017) An integrated model of phenotypic trait changes and site-specific sequence evolution. *Syst. Biol.*, **66**, 917–933.
- Schneider, T., Smith, G.H., Rossi, M.R., Hill, C.E. and Zhang, L. (2018) Validation of a customized bioinformatics pipeline for a clinical next-generation sequencing test targeting solid tumor-associated variants. *J. Mol. Diagn.*, **20**, 355–365.
- Guo, Y., Li, J., Li, C.-I., Long, J., Samuels, D.C. and Shyr, Y. (2012) The effect of strand bias in illumina short-read sequencing data. *BMC Genomics*, **13**, 666.
- Allhoff, M., Schönhuth, A., Martin, M., Costa, I.G., Rahmann, S. and Marschall, T. (2013) Discovering motifs that induce sequencing errors. *BMC Bioinformatics*, **14**(Suppl. 5), S1.
- Loman, N.J., Misra, R.V., Dallman, T.J., Constantinidou, C., Gharbia, S.E., Wain, J. and Pallen, M.J. (2012) Performance comparison of benchtop high-throughput sequencing platforms. *Nat. Biotechnol.*, **30**, 434–439.
- Marinier, E., Brown, D.G. and McConkey, B.J. (2015) Pollux: platform independent error correction of single and mixed genomes. *BMC Bioinformatics*, **16**, 10.
- Minoche, A.E., Dohm, J.C. and Himmelbauer, H. (2011) Evaluation of genomic high-throughput sequencing data generated on illumina hiseq and genome analyzer systems. *Genome Biol.*, **12**, R112.
- Quail, M.A., Smith, M., Coupland, P., Otto, T.D., Harris, S.R., Connor, T.R., Bertoni, A., Swerdlow, H.P. and Gu, Y. (2012) A tale of three next generation sequencing platforms: comparison of ion torrent, pacific biosciences and illumina miseq sequencers. *BMC Genomics*, **13**, 341.
- Ross, M.G., Russ, C., Costello, M., Hollinger, A., Lennon, N.J., Hegarty, R., Nusbaum, C. and Jaffe, D.B. (2013) Characterizing and measuring bias in sequence data. *Genome Biol.*, **14**, R51.

42. Luo,C., Tsementzi,D., Kyrpides,N., Read,T. and Konstantinidis,K.T. (2012) Direct comparisons of illumina vs. Roche 454 sequencing technologies on the same microbial community DNA sample. *PLoS One*, **7**, e30087.
43. Stoler,N. and Nekrutenko,A. (2021) Sequencing error profiles of illumina sequencing instruments. *NAR Genom. Bioinform*, **3**, lqab019.
44. McNaughton,A.L., Roberts,H.E., Bonsall,D., de Cesare,M., Mokaya,J., Lumley,S.F., Golubchik,T., Piazza,P., Martin,J.B., de Lara,C. *et al.* (2019) Illumina and nanopore methods for whole genome sequencing of hepatitis b virus (HBV). *Sci. Rep.*, **9**, 7081.
45. Schirmer,M., D'Amore,R., Ijaz,U.Z., Hall,N. and Quince,C. (2016) Illumina error profiles: resolving fine-scale variation in metagenomic sequencing data. *BMC Bioinformatics*, **17**, 125.
46. Caboche,S., Audebert,C. and Lemoine,Y. Hot,D. (2014) Comparison of mapping algorithms used in high-throughput sequencing: application to ion torrent data. *BMC Genomics*, **15**, 264.